Journal of Power Sources 221 (2013) 90–96

Contents lists available at SciVerse ScienceDirect

Journal of Power Sources

journal homepage: www.elsevier.com/locate/jpowsour

Tris(trimethylsilyl) borate as an electrolyte additive to improve the cyclability of $LiMn_2O_4$ cathode for lithium-ion battery

Yanbo Liu, Lei Tan, Lei Li*

School of Chemistry and Chemical Engineering, Shanghai Jiaotong University, Shanghai 200240, China

HIGHLIGHTS

► TMSB used as additive to improve cyclability of $LiMn_2O_4$ cathode lithium-ion battery.
► The lithium-ion battery containing TMSB shows excellent capacity retention at 55 °C.
► TMSB participated in the formation of SEI on the surface of electrode.
► Enhancement of cyclability of Li anode by TMSB additive.

ARTICLE INFO

Article history:
Received 4 June 2012
Received in revised form
28 June 2012
Accepted 13 August 2012
Available online 21 August 2012

Keywords:
Electrolyte additive
Lithium-ion battery
Tris(trimethylsilyl) borate
Lithium manganese oxide
Cycle life

ABSTRACT

In order to overcome severe capacity fading of $LiMn_2O_4$ cathode lithium-ion battery, tris(trimethylsilyl) borate (TMSB) is used as an electrolyte additive. With 0.5 wt% TMSB addition into the electrolyte (EC/DMC with 1 M $LiPF_6$), the capacity retention is significantly improved at both room temperature and 55 °C. The effects of the TMSB on the $LiMn_2O_4$ electrode are investigated via a combination of cyclability, capacity retention of high temperature storage, electrochemical impedance spectroscopy (EIS), scanning electron microscope (SEM), X-ray photoelectron spectroscopy (XPS) and X-ray diffraction (XRD). Based on these results, it is suggested that the improved cyclability of the cells containing the TMSB additive is mainly originated from the participation in the formation of solid electrolyte interface (SEI) on the surface of electrode, the dissolution of LiF out of the SEI and the enhancement of cyclability of Li anode.

1. Introduction

During the past few decades, lithium-ion batteries (LIBs) have been developed as the power source for electric vehicles (EVs) and plug-in hybrid electric vehicles (HEVs) [1,2], which generally require a long cycle life and high capacity retention. As the performance, price, and safety of lithium-ion batteries mainly depend on the properties of the cathode materials, much attention has been paid to the search for high capacity, cheap and safe cathode materials [1,2]. Among all candidate cathode materials, $LiMn_2O_4$ becomes the promising cathode material for commercial usage due to the low cost, safety, cyclability and benign to environment. However, the batteries used spinel $LiMn_2O_4$ as cathode material have problems with severe capacity fading and poor cycling, especially at elevated temperature [3–6]. The main reason for capacity fading is the dissolution of Mn^{2+} from spinel $LiMn_2O_4$ into electrolyte due to the presence of HF, which is formed by the decomposition of lithium hexafluorophosphate ($LiPF_6$) salt with residual water in the electrolyte [7–10]. In order to suppress Mn^{2+} dissolution, material scientists are doing many endeavor to develop new stable $LiMn_2O_4$ materials by using different methods: (1) partial Mn substitution with different transition metals, (2) partial anion substitution O with F, and (3) metal oxide surface coatings [11]. However, the improvement of the electrode materials involves complex synthetic process and high cost.

The use of electrolyte additives would be one of the most effective and economic methods to suppress the capacity fading and improve the cycling performance of $LiMn_2O_4$ lithium-ion batteries. Usually, the amount of an electrolyte additive is no more than 5 wt% while its presence significantly improves the cyclability of LIBs. Sun et al. [12] reported tris(pentafluorophenyl) borane (TPFPB) as an anion receptor electrolyte additive for

* Corresponding author. Tel.: +86 21 34202613; fax: +86 54742567.
E-mail address: lilei0323@sjtu.edu.cn (L. Li).

0378-7753/$ – see front matter © 2012 Elsevier B.V. All rights reserved.
http://dx.doi.org/10.1016/j.jpowsour.2012.08.028

$LiMn_2O_4$/Li battery. The $LiMn_2O_4$/Li battery with the $LiPF_6$-based electrolyte containing 0.1 M TPFPB additive exhibited more superior capacity retention and coulomb efficiency at 55 °C than the battery without additive. Park et al. [13] used fluoroethylene carbonate (FEC) as an electrolyte additive to improve the capacity retention of $LiMn_2O_4$/graphite LIBs. With 2 wt% FEC addition into the electrolyte (EC/DEC/PC with 1 M $LiPF_6$), the capacity retention at 60 °C after 130 cycles was significantly improved by about 20%. The heptamethyldisilazane used as an additive to improve the stability of the electrolyte (EC/EMC/PC with 1 M $LiPF_6$) and cycling performance of $LiMn_2O_4$ batteries was also reported [14].

In this paper, tris(trimethylsilyl) borate (TMSB), was used as electrolyte additive to improve the performance of $LiMn_2O_4$/Li battery with 1 M $LiPF_6$ in EC/DMC (1:1, w:w). The effects of TMSB on the improvement of electrolyte thermal stability and cycle life of the $LiMn_2O_4$/Li battery were investigated.

2. Experimental

Battery-grade ethylene carbonate (EC), dimethyl carbonate (DMC) and $LiPF_6$ were purchased from Shenzhen Capchem Chemicals Co., Ltd., China, and used without further purification. Battery-grade tris(trimethylsilyl) borate was purchased from Fujian Chuangxin Science and Technology Develops Co., Ltd., China, and used without further purification. The electrolytes of 1 M $LiPF_6$ in a 1:1 (weight ratio) EC/DMC with and without 0.5 wt% TMSB additive were prepared in an argon-filled glove box, in which the oxygen and water content were less than 1 ppm.

$LiMn_2O_4$ cathode materials were purchased from Hunan Reshine New Material Co., Ltd., China. The $LiMn_2O_4$ electrodes were prepared by mixing the $LiMn_2O_4$ powder (90 wt%), carbon black (5 wt%) and poly(vinylidene fluoride) (PVDF 5 wt%) in N-methyl-pyrrolidone (NMP) solvent. The mixed slurry was coated onto aluminum foil and dried at 80 °C for 0.5 h, then dried at 125 °C at 1.5 h. The dried electrode was then compressed by a roller to make a compact and smooth film structure at room temperature. The electrode disks (1.5386 cm^2) were then punched out of the coated foil sheets and weighted. $LiMn_2O_4$/Li half cells were fabricated with 2016-coin type cells in the argon-filled glove box using Celgard 2400 as the separator.

The charge–discharge behavior of the cells was tested on Land CT2001A tester (Wuhan, China) at the constant current mode over the range of 3.0–4.5 V. The constant current mode of 1.0 C was carried out at both room temperature and 55 °C. At the initial and last cycled galvanostatic measurement, electrochemical impedance spectroscopy (EIS) of the cell was observed immediately under full charged condition. EIS measurement was accomplished by coupling the potentiostat with an Autolab frequency response analyzer locked in an amplifier and an impedance phase analyzer. A sinusoidal amplitude modulation was used over the frequency range from 0.1 Hz to 1 MHz.

The storage test of the $LiMn_2O_4$/Li cells at 80 °C was carried out followed by the procedure: the assembled cells were charged with a constant current of 0.5 C–4.5 V, and then the full charged cells were put into an oven at 80 °C for 24 h, 48 h and 72 h, respectively. After that, the full charged cells were discharged to 3.0 V at room temperature. The tested cells were all under the full-charged status.

The lithium cycling performance was carried out by using sealed 2016-coin type Li/stainless steel cells at 55 °C in our experiments. The electrolytes of 1 M $LiPF_6$ in a 1:1 (weight ratio) EC/DMC with and without 0.5 wt% TMSB additive were used. The electrodes were separated by Celgard 2400 film. An excess of lithium (3.6 C cm^{-2}) was first galvanostatically plated on the surface of the stainless steel electrode, and then consumed by galvanostatic cycling of a fraction of the original excess lithium (0.36 C cm^{-2}). The experiment was stopped as a sharp change in dissolution potential (0.3 V *vs.* Li/Li^+) happened.

To analyze the element composition and microstructure of the $LiMn_2O_4$ electrodes after charge–discharge cycling measurements, the cells were disassembled in an argon-filled glove box. The $LiMn_2O_4$ electrodes were washed with anhydrous DMC several times to remove residual salts, and then dried in vacuum oven for 2 h at room temperature. Scanning electron microscope (SEM, Ultra 55, Carl Zeiss) was used to observe the morphology of the $LiMn_2O_4$ electrodes. X-ray diffraction (XRD) patterns were recorded at room temperature using a X-ray diffractometer (XRD, D/max-2200/PC, Japan) by continuous scanning in the 2θ range of 5–80°. X-ray photoelectron spectroscopy (XPS) measurements were carried out by a Kratos Axis UltraDLD spectrometer (Kratos Analytical-A Shimadzu group company) using a monochromatic Al Kα radiation ($h\gamma$ = 1486.6 eV). The analyzer used hybrid magnification mode (both electrostatic and magnetic) and the take-off angle was 90°. The pass energy was fixed at 40.0 eV to ensure high resolution and sensitivity. Binding energy was calibrated by using the containment carbon (C1s = 2 84.8 eV). Peak assignment was made based on detailed curve fitting of the recorded spectra using Gaussian-Gauss2 peak shapes and a Shirley function background correction. The Kratos charge neutralizer system was used on all specimens except the conductive samples.

3. Results and discussion

The $LiMn_2O_4$/Li half cells were assembled containing 1 M $LiPF_6$ in EC/DMC (1:1, w:w) composite electrolytes without and with the presence of 0.5 wt% TMSB additive. The cells were cycled at 1.0 C rate under constant current conditions. The experiments were carried out at both room temperature and 55 °C. Fig. 1 shows the cycle performance of the $LiMn_2O_4$/Li cells at room temperature with different electrolytes. The cell with conventional electrolyte displayed about 23% capacity loss at the 180th cycle, while the cell containing 0.5 wt% TMSB additive showed only 5% capacity loss at the same cycle number. Fig. 2 shows coulombic efficiency (CE) of these cells. It can be found that both the cells exhibited a very high CE over 180 cycles. And the cell containing the TMSB additive exhibited a higher CE than that of the cell with the conventional electrolyte. The higher CE and less fluctuation of CE during the

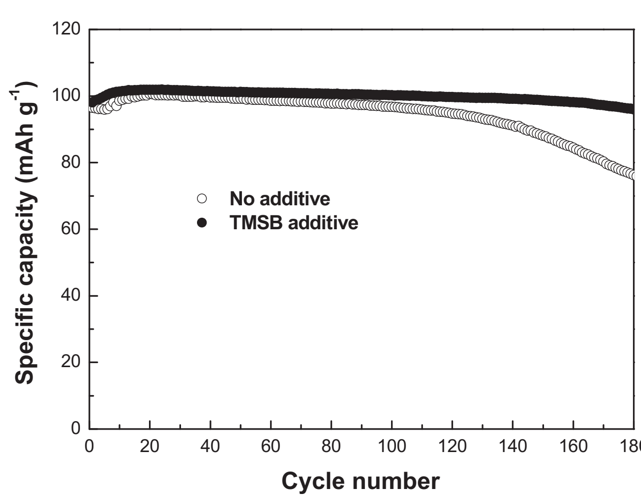

Fig. 1. Cycle performance of $LiMn_2O_4$/Li half cells using 1 M $LiPF_6$ in EC/DMC (1:1, w:w) as electrolytes with and without 0.5 wt% TMSB additive at room temperature. Charge–discharge rate was 1.0 C in the potential range of 3.0–4.5 V.

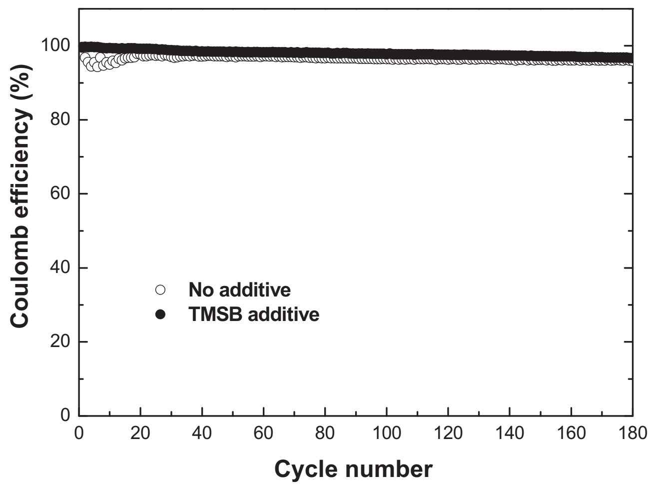

Fig. 2. Coulomb efficiency of $LiMn_2O_4$/Li half cells using 1 M $LiPF_6$ in EC/DMC (1:1, w:w) as electrolytes with and without 0.5 wt% TMSB additive at room temperature.

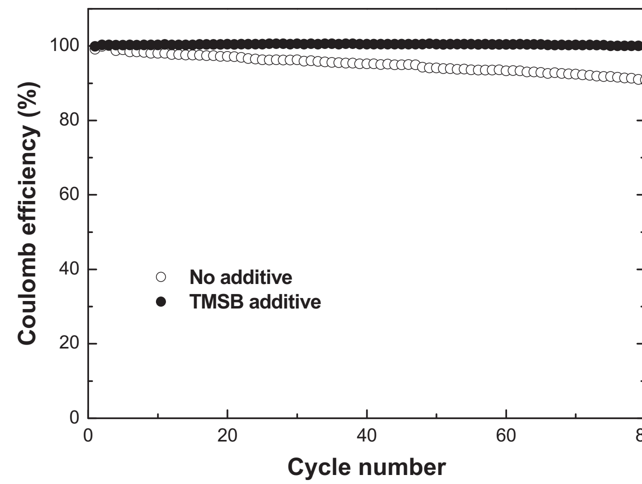

Fig. 4. Coulomb efficiency of $LiMn_2O_4$/Li half cells using 1 M $LiPF_6$ in EC/DMC (1:1, w:w) as electrolytes with and without 0.5 wt% TMSB additive at 55 °C.

cycling of the cell containing the TMSB additive indicate that the TMSB additive will affect the formation of the solid electrolyte interface (SEI) layer in a favorable way.

Fig. 3 compares the variation of capacity *vs*. cycle number obtained from the cells with the different electrolytes at 55 °C. The cell with the conventional electrolyte displayed about 18% capacity loss at the 80th cycle, while the cell containing 0.5 wt% TMSB additive showed less than 3% capacity loss at the same cycle number. The cells with the composite electrolyte containing 0.5 wt% TMSB additive exhibit more stable cycle performance than the cells with the conventional electrolyte, especially at elevated temperature. The CEs of these cells are shown in Fig. 4. It can be observed that the cell containing the TMSB additive exhibited a higher CE than that of the cell with the conventional electrolyte. The CE of the cell containing 0.5 wt% TMSB additive was about 99.9% at the 80th cycle, while the CE of the cell with the conventional electrolyte was about 90.9% at the same cycle number. These results indicate that the TMSB additive maintained excellent cycle performance of the $LiMn_2O_4$/Li cells. In order to understand the sources of the difference in capacity retention, AC impedance, surface analysis of these $LiMn_2O_4$ electrodes were carried out as described below.

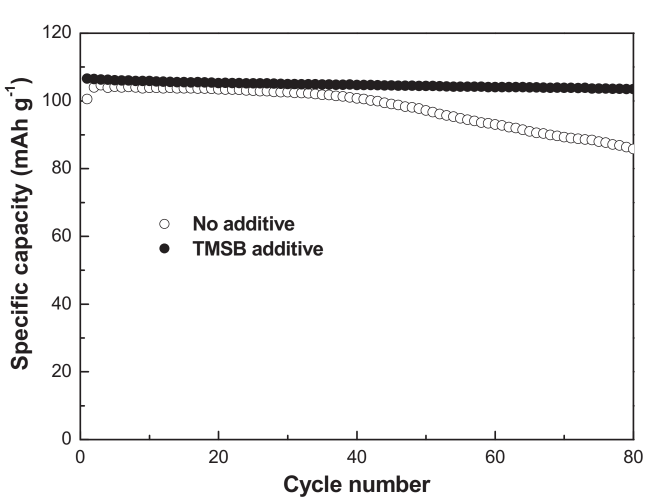

Fig. 3. Cycle performance of $LiMn_2O_4$/Li half cells using 1 M $LiPF_6$ in EC/DMC (1:1, w:w) as electrolytes with and without 0.5 wt% TMSB additive at 55 °C. Charge–discharge rate was 1.0 C in the potential range of 3.0–4.5 V.

AC impedance data of the $LiMn_2O_4$/Li half cells with different composite electrolytes are shown in Fig. 5. The AC impedance was measured after the cells were full charged. Generally, the EIS impedance of the cells consisted of electrolyte resistance (R_e), SEI resistance (R_f) and charge transfer resistance (R_{ct}). From Fig. 5a, it is clearly found that the interfacial impedances of the cells, which consisted of R_f and R_{ct}, were not markedly changed for both cells with and without TMSB additive after the formation cycles at room temperature. After 180th cycles at room temperature, however, the electrolyte resistance (R_e) of the cell with TMSB additive (8.82 Ω) was smaller than that of the cell without additive (16.79 Ω), and R_f of the cell with TMSB additive (4.17 Ω) was significantly smaller than that of the cell without additive (32.49 Ω). After 80th cycles at 55 °C, R_e of both cells with TMSB and without additive made no obvious difference, however, R_f of the cell with TMSB additive (7.15 Ω) was significantly smaller than that of the cell without additive (22.73 Ω). The similar behaviors were also found in the $LiFePO_4$ cathode lithium-ion batteries [15].

The surfaces of the $LiMn_2O_4$ electrodes after 80 cycles at 55 °C with the different electrolytes were analyzed by XPS. The C1s, O1s, F1s, B1s, Si2p, and Mn2p spectra of both electrodes are shown in Fig. 6. The C1s spectra show slight differences between the cathode cycled without additive and with 0.5 wt% TMSB additive (see Fig. 6a). There are four characteristic peaks in the C1s spectra: C–C bond in carbon black (284.1 eV) [16], C–H bond in lithium alkyl carbonates ($R-CH_2OCO_2-Li$) or PVDF (286.0 eV) [17], C=O bond in lithium alkyl carbonates ($R-CH_2OCO_2-Li$) or polycarbonates (289.6 eV) [16], as well as Li_2CO_3 (290.5 eV) [16,17]. The intensities of C–H and C=O bonds observed on the surface of the $LiMn_2O_4$ electrode cycled with the TMSB additive are much stronger than that of the cathode cycled without additive. This indicates that more $R-CH_2OCO_2-Li$ or polycarbonates were formed on the surface of the $LiMn_2O_4$ electrode containing the TMSB additive, which will improve the transportation of lithium ion. In addition, the intensity of Li_2CO_3 observed on the surface of the $LiMn_2O_4$ electrode cycled with the TMSB additive is lower than that of the cathode cycled without additive. This suggests that the electrode cycled with the conventional electrolyte was covered with more Li_2CO_3, inorganic degradation products, than that of the electrode cycled containing the TMSB additive.

There are four main peaks in the O1s spectra shown in Fig. 6b, dominated by Mn–O bond in Mn_xO_y or $LiMn_2O_4$ (529.6 eV) [17], C=O bond in lithium alkyl carbonates ($R-CH_2OCO_2-Li$) or ethers (531.3 eV) [17], Li_2CO_3 (532.0 eV) [18], as well as C–O bond in

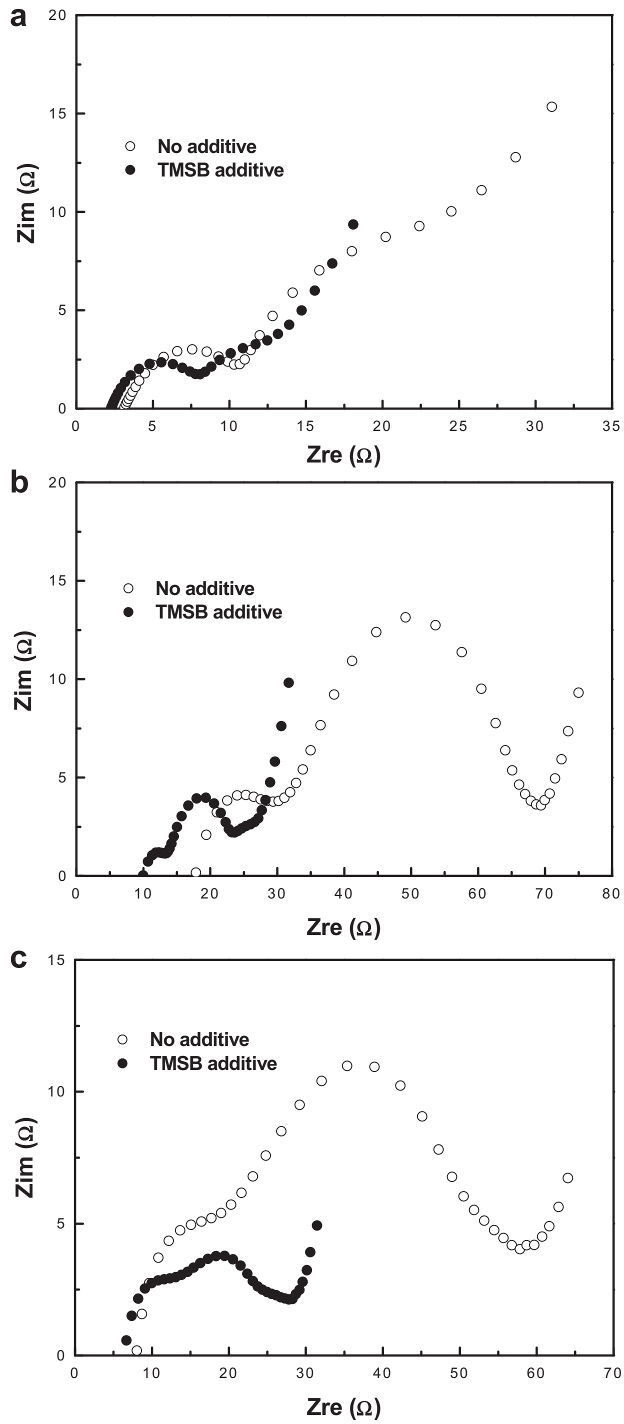

Fig. 5. Impedance spectra of full charged $LiMn_2O_4$/Li half cells using 1 M $LiPF_6$ in EC/DMC (1:1, w:w) as electrolytes with and without 0.5 wt% TMSB additive: (a) after first 1.0 C charged cell at room temperature (b) after 180 cycles 1.0 C charge–discharged cell at room temperature (c) after 80 cycles 1.0 C charge–discharged cell at 55 °C. Frequency range: 0.1–1 MHz.

lithium alkyl carbonates ($R-CH_2OCO_2-Li$) or polycarbonates (533.3 eV) [17]. The intensities of Mn–O and Li_2CO_3 observed on the surface of the $LiMn_2O_4$ electrode cycled without additive are stronger than that of the cathode cycled with 0.5 wt% TMSB. This suggests that the $LiMn_2O_4$ cathode electrode cycled without additive was covered with more inorganic degradation products, such as Mn_xO_y and Li_2CO_3, than that of the $LiMn_2O_4$ cathode electrode cycled with 0.5 wt% TMSB. The intensities of C–O and C=O bonds observed on the surface of the $LiMn_2O_4$ electrode cycled with 0.5 wt% TMSB are stronger than that of the cathode cycled without additive, which indicates that more $R-CH_2OCO_2-Li$ or polycarbonates were formed on the surface of the $LiMn_2O_4$ electrode.

The F1s spectra shows obvious differences between the cathode cycled without additive and with 0.5 wt% TMSB additive (see Fig. 6c). The F1s spectra contain four main peaks: LiF (685.3 eV) [19], $LiP_xO_yF_z$ (687.0 eV) [18], PVDF (687.6 eV) [18] and LiP_xF_y (688.3 eV) [18]. The intensity of LiF of the $LiMn_2O_4$ electrode extracted from the cell cycled without additive is much stronger than that of the cathode cycled with TMSB additive, suggesting more inorganic products covered on the surface of the electrode with the conventional electrolyte, which consistent with the C1s and O1s spectra as discussed above.

Based on these XPS analytical results on the C1s, O1s and F1s spectra, it can be found that more inorganic degradation products such as Mn_xO_y, Li_2CO_3 and LiF were covered on the $LiMn_2O_4$ electrode with the conventional electrolyte compared with the electrode containing the TMSB additive. From SEM measurements shown in Fig. 7, it can be found that there are more fluff-like and particle-like materials, inorganic degradation products, covered onto the surface of the electrode with the conventional electrolyte (see Fig. 7b) compared with the pristine electrode (see Fig. 7a). In addition, it can be found that the morphology of the $LiMn_2O_4$ electrode cycled with 0.5 wt% TMSB additive shown in Fig. 7c shows similar to the morphology of the pristine electrode. Since the TMSB is an electron-deficient boron compound, it can easily be combined with some electron-rich materials such as F^-. It is well known that the LiF is a nonconductor for both electrons and lithium ions, hence the formed LiF onto the electrodes will result in increasing the interfacial impedance of the cells (see Fig. 5). The combination of TMSB-F^- will improve the dissolvability of the LiF in the electrolyte. Therefore, the dissolution of the LiF from the passivation film can result in lower interfacial impedance. In addition, more $R-CH_2OCO_2-Li$ or polycarbonates were formed on the surface of the $LiMn_2O_4$ electrode, which will also improve the transportation of lithium ion. Based on these effects, it results in the cell resistance in the electrolyte containing the TMSB additive was smaller than that with the conventional electrolyte.

The Mn2p spectra of the electrodes after 80 cycles at 55 °C were shown in Fig. 6d. There are three main peaks in Mn2p spectra, dominated by $Mn2p^{3/2}$: Mn^{3+} in Mn_2O_3 or $LiMn_2O_4$ (641.7 eV), Mn^{4+} in MnO_2 or $LiMn_2O_4$ (642.9e V), and $Mn2p^{1/2}$ (653.6 eV) [20]. Both the peak position and the intensity ratio of $Mn2p^{3/2}$ and $Mn2p^{1/2}$ showed that the $LiMn_2O_4$ existed in a stoichiometric spinel form. The intensities of both Mn^{3+} and Mn^{4+} peaks observed on the surface of the $LiMn_2O_4$ electrode cycled with 0.5 wt% TMSB additive are stronger than that of the electrode cycled without additive.

To further confirm the fact that TMSB participated in the formation of SEI on the surface of the $LiMn_2O_4$ electrode, both the Si2p and B1s spectra of the electrode with TMSB additives were measured (see Fig. 6e). It is clearly observed that there is one main peak in the Si2p spectra dominated by C–O–Si bond (102.0 eV) [21] and two main peaks in the B1s spectra. These results indicate that the TMSB additives participated in the formation of SEI. The improvement of SEI will reduce the dissolution of Mn^{2+} into electrolyte, which resulted in good cycle performance of the battery cycled with 0.5 wt% TMSB to a large extent. The similar results on the improvement of the cyclability and capacity retention of lithium-ion batteries were also reported with using some boron compounds as electrolyte additives such as tris(pentafluorophenyl) borate (TPFPB) and Lithium bis(oxalato) borate [22,23].

Fig. 8 shows the XRD patterns of the pristine and $LiMn_2O_4$ electrodes after 80 cycles with and without 0.5 wt% TMSB additive at

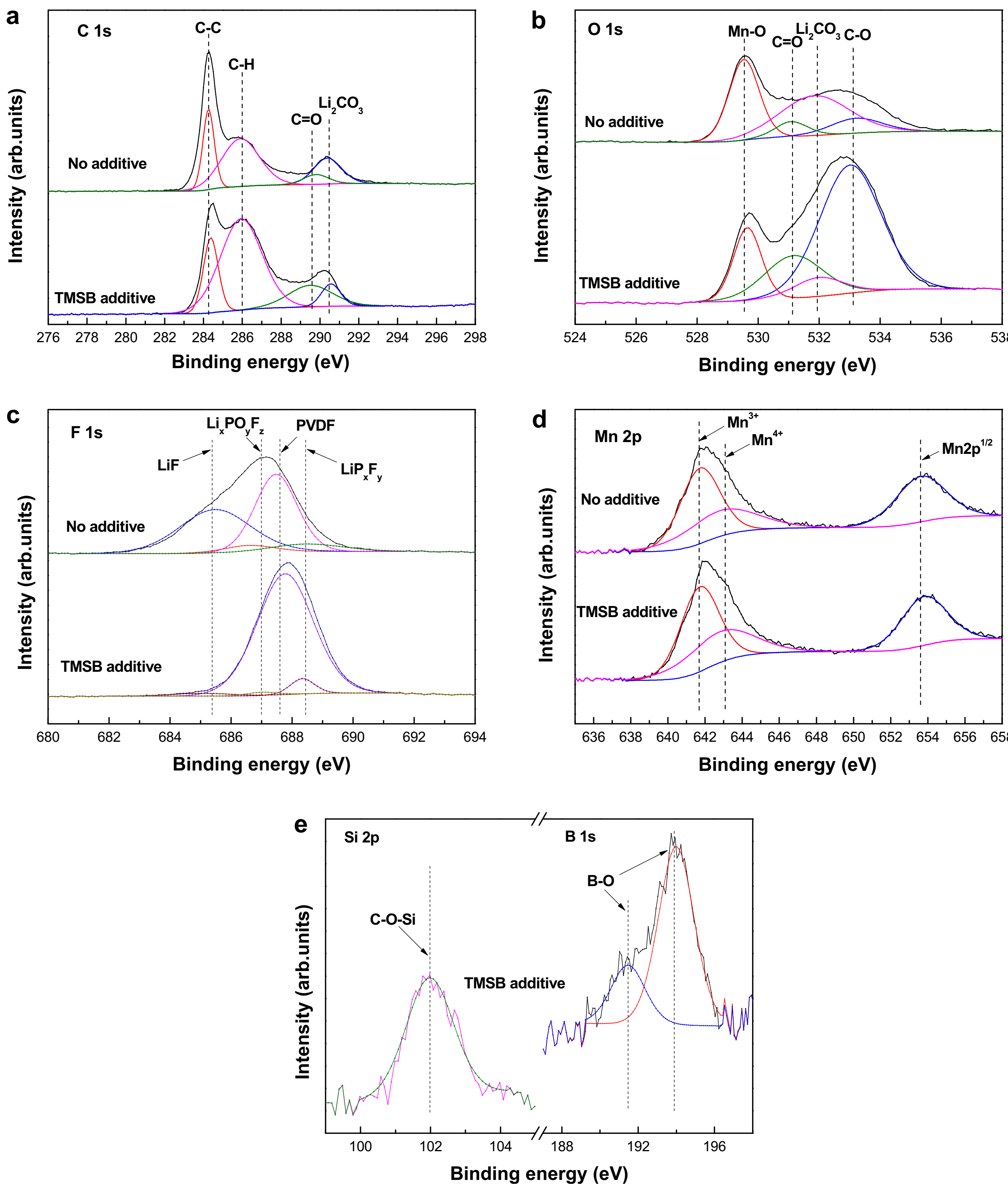

Fig. 6. XPS spectra of $LiMn_2O_4$ electrodes after 80 cycles at 55 °C. (a) C1s spectra, (b) O1s spectra, (c) F1s spectra, (d) Mn2p spectra, (e) Si2p and B1s spectra.

55 °C. All the peaks in the XRD patterns of the $LiMn_2O_4$ electrode were indexed as the spinel phase (JCPDS file No. 35-0782). Compared with the pristine electrode, however, the intensities of all the $LiMn_2O_4$ diffraction peaks of the electrodes are weakened. This is may be due to the decay of the spinel structure of $LiMn_2O_4$ which resulted from Mn^{2+} dissolution at elevated temperature [7–10]. However, the extent of weakening of the electrode without TMSB additive is stronger than that of the electrode with TMSB additive. Fig. 8b shows the magnified patterns at $2\theta = 17–37°$. It can be found that both the diffraction peaks (111) and (311) of the electrode without additive shifted to higher angle after cycled, suggesting the shrinkage of the crystal lattice [24]. However, no obvious shift was found in the diffraction peaks of the electrode with the TMSB additive even after 80 cycles. These results indicate that the extent of

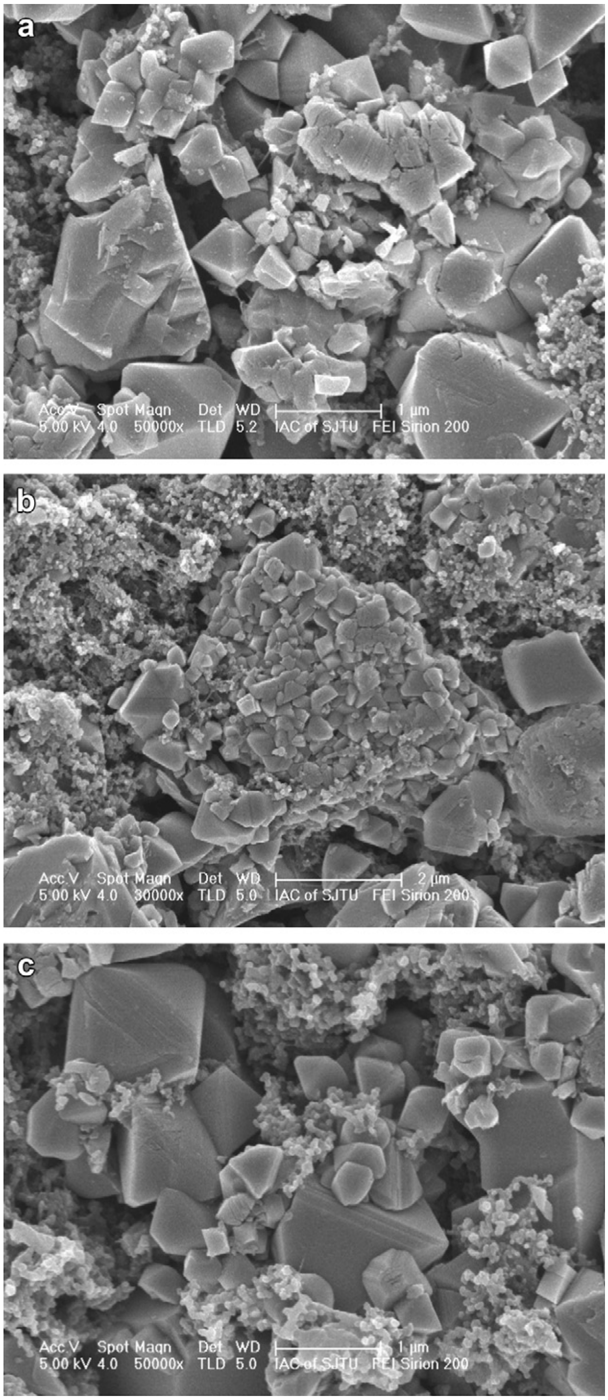

Fig. 7. SEM micrographs of $LiMn_2O_4$ electrodes: (a) pristine electrode, and electrodes after 80 cycles at 55 °C using 1 M $LiPF_6$ in EC/DMC (1:1, w:w) as electrolytes without (b) and with (c) 0.5 wt% TMSB additive.

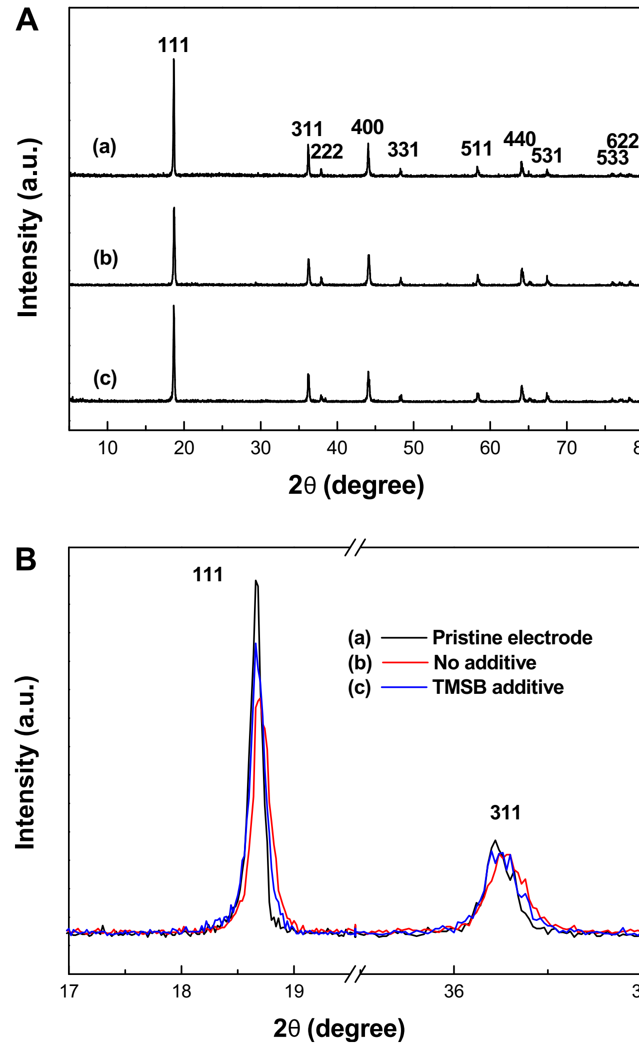

Fig. 8. XRD patterns of $LiMn_2O_4$ electrodes (A) and the magnified between 17 and 37 for 2θ (B): (a) pristine electrode, and electrodes after 80 cycles at 55 °C with 1 M $LiPF_6$ in EC/DMC (1:1, w:w) as electrolytes without (b) and with (c) 0.5 wt% TMSB additive.

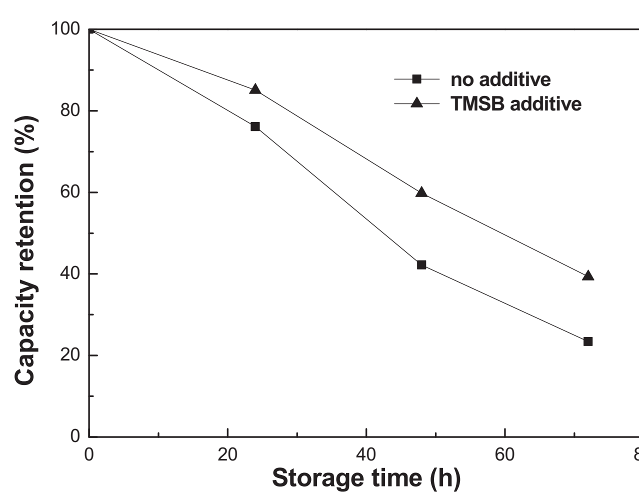

Fig. 9. Capacity retention of Li/$LiMn_2O_4$ half cells after storage at 80 °C for different times.

degradation of the spinel structure of $LiMn_2O_4$ in the electrode without additive is much stronger than that of the electrode containing the TMSB additive, which is consistent with the Mn2p spectra as discussed above.

In order to the effect of TMSB to $LiPF_6$-based electrolyte, a high temperature storage test of the cells without and with TMSB additives was carried out at 80 °C in our experiments. From Fig. 9, it can be found that the capacity retention of both the cells significant reduced with increasing the storage time. However, the cell with

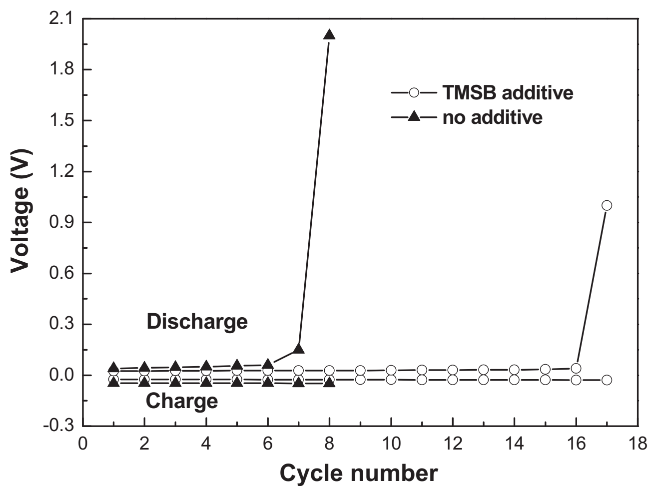

Fig. 10. The voltage change of lithium deposition–dissolution on stainless steel substrates with cycle number in different electrolytes. Temperature: 55 °C.

TMSB additive showed higher capacity retention than that of the cell without additive. The improvement of the capacity retention at high temperature may be that the TMSB additive participated in the formation of SEI on the surface of the $LiMn_2O_4$ electrode, which then reduce the side reactions with electrolytes.

To further confirm the effect of the TMSB additive on the cycle performance of Li anode, the lithium cycling performance was carried out by using a Li/Stainless Steel (Li/SS) cells in our experiments. Before these experiments, anode, the Li/SS cells were discharged with a constant current 0.4 mA for 5 h to make sure that a certain amount of Li (3.6 C cm^{-2}) was deposited onto the stainless steel electrode, and then a fraction of the original excess lithium (0.36 C cm^{-2}) was transported every cycle till the deposited original excess lithium was consumed. The voltage of lithium deposition–dissolution on the stainless steel electrode ended up with more and more obvious polarization. The cycling performance of the cell with TMSB additive was obviously better than that of the cell without additive (see Fig. 10). These results indicate that the enhancement of cyclability of Li anode by TMSB additive is also one of the reasons to improve the cyclability of the $LiMn_2O_4$/Li cells (see Figs. 1–4).

4. Conclusion

It has been proved that the TMSB can be used as an effective electrolyte additive to improve the cycle life of $LiMn_2O_4$ cathode lithium-ion battery. The capacity fading of the cells was obviously reduced when 0.5 wt% TMSB was added into the conventional electrolyte, 1 M $LiPF_6$ in EC/DMC (1:1, w:w). At 55 °C, the cell with the conventional electrolyte displayed about 18% capacity loss at the 80th cycle, while the cell containing 0.5 wt% TMSB additive showed less than 3% capacity loss at the same cycle number. EIS indicates that the interfacial impedance of the cell cycled with 0.5 wt% TMSB is much lower than the cell cycled without additive at both room temperature and 55 °C. The mechanism of the enhanced performance of the $LiMn_2O_4$/Li cells has been investigated by XPS, SEM and XRD. It was found that there are several reasons for the improvement of cycle performance of the $LiMn_2O_4$/Li cell with TMSB additive: (1) the coordination of TMSB-F^- compound, which will dissolve LiF out of the SEI, (2) the participation of TMSB in the formation of SEI on the surface of the electrode, (3) the enhancement of cyclability of Li anode by TMSB additive. Therefore, the TMSB is an effective electrolyte additive to improve the cycling performance of $LiMn_2O_4$ cathode for lithium-ion battery.

Acknowledgments

The work was supported by the National Natural Science Foundation of China (Grant No.20904031) and the Shanghai Leading Academic Discipline Project (No. B202). Thanks for Instrumental Analysis Center of Shanghai Jiaotong University.

References

[1] J.M. Tarascon, M. Armand, Nature 414 (2001) 359–367.
[2] M. Armand, J.M. Tarascon, Nature 451 (2008) 652–657.
[3] A. Blyr, C. Sigala, G. Amatucci, D. Guyomard, Y. Chabre, J.M. Tarascon, J. Electrochem. Soc. 145 (1998) 194–209.
[4] A.D. Pasquier, A. Blyr, P. Courjal, D. Larcher, G. Amatucci, B. Gerand, J.M. Tarascon, J. Electrochem. Soc. 146 (1999) 428–436.
[5] Y.Y. Xia, T. Sakai, T. Fujieda, X.Q. Yang, X. Sun, Z.F. Ma, J. McBreen, M. Yoshio, J. Electrochem. Soc. 148 (2001) 723–729.
[6] J. Shim, R. Kostecki, T. Richardson, X. Song, K.A. Striebel, J. Power Sources 112 (2002) 222–230.
[7] C.J. Curtis, J.X. Wang, D.L. Schulz, J. Electrochem. Soc. 151 (2004) 590–598.
[8] N. Kumagai, S. Komaba, Y. Kataoka, M. Koyanagi, Chem. Lett. 29 (2000) 1154–1155.
[9] H. Yamane, M. Saitoh, M. Sano, M. Fujita, M. Takada, E. Nishibori, N. Tanaka, J. Electrochem. Soc. 149 (2002) 1514–1520.
[10] J.B. Goodenough, J. Power Sources 174 (2007) 996–1000.
[11] Z. Chen, K. Amine, J. Electrochem. Soc. 153 (2006) 316–320.
[12] X. Sun, H.S. Lee, X.Q. Yang, J. McBreen, Electrochem. Solid-State Lett. 5 (2002) 248–251.
[13] M.-H. Ryou, G.-B. Han, Y.M. Lee, J.-N. Lee, D.J. Lee, Y.-O. Yoon, J.-K. Park, Electrochim. Acta 55 (2010) 2073–2077.
[14] Y. Li, R. Zhang, J. Liu, C. Yang, J. Power Sources 189 (2009) 685–688.
[15] Z.J. Cai, Y.B. Liu, J.H. Zhao, L. Li, Y.M. Zhang, J. Zhang, J. Power Sources 202 (2012) 341–346.
[16] M.Q. Xu, L.S. Hao, Y.L. Liu, W.S. Li, L.D. Xing, B. Li, J. Phys. Chem. C 115 (2011) 6085–6094.
[17] Y. Kusachi, Z.C. Zhang, J. Dong, K. Amine, J. Phys. Chem. C 115 (2011) 24013–24020.
[18] L. Zhou, S. Dalavi, M.Q. Xu, B. Lucht, J. Power Sources 196 (2011) 8073–8084.
[19] M. Balasubramanian, H.S. Lee, X. Sun, X.Q. Yang, A.R. Moodenbaugh, J. McBreen, D.A. Fischer, Z. Fu, Electrochem. Solid-State Lett. 5 (2002) 22–25.
[20] N. Treuil, C. Labrugere, M. Menetrier, J. Portier, G. Campet, A. Deshayes, J.C. Frison, S.J. Hwang, S.W. Song, J.H. Choy, J. Phys. Chem. B 103 (1999) 2100–2106.
[21] J.S. Kim, W.C. Choi, D.J. Byun, J.K. Lee, Solid State Ionics 212 (2012) 43–46.
[22] S.S. Zhang, J. Power Sources 162 (2006) 1379–1394.
[23] S.S. Zhang, K. Xu, T.R. Jow, Electrochem. Solid-State Lett. 5 (2002) 206–208.
[24] Y.J. Liu, X.H. Li, H.J. Guo, Z.X. Wang, Q.Y. Hu, W.J. Peng, Y. Yang, J. Power Sources 189 (2009) 721–725.